

# Unfolding DNA condensates produced by DNA-like charged depletants: A force spectroscopy study

C. H. M. Lima, M. S. Rocha, and E. B. Ramos

Citation: *The Journal of Chemical Physics* **146**, 054901 (2017); doi: 10.1063/1.4975103

View online: <https://doi.org/10.1063/1.4975103>

View Table of Contents: <http://aip.scitation.org/toc/jcp/146/5>

Published by the [American Institute of Physics](#)

---

## Articles you may be interested in

[Nematic-like stable glasses without equilibrium liquid crystal phases](#)

*The Journal of Chemical Physics* **146**, 054503 (2017); 10.1063/1.4974829

[Highly driven polymer translocation from a cylindrical cavity with a finite length](#)

*The Journal of Chemical Physics* **146**, 054903 (2017); 10.1063/1.4975091

[Extremely asymmetric phase diagram of homopolymer-monotethered nanoparticles: Competition between chain conformational entropy and particle steric interaction](#)

*The Journal of Chemical Physics* **146**, 054902 (2017); 10.1063/1.4975023

[Statistical-thermodynamic model for light scattering from eye lens protein mixtures](#)

*The Journal of Chemical Physics* **146**, 055101 (2017); 10.1063/1.4974155

[Size dependent tunnel diode effects in gold tipped CdSe nanodumbbells](#)

*The Journal of Chemical Physics* **146**, 054703 (2017); 10.1063/1.4975102

[Water graphene contact surface investigated by pairwise potentials from force-matching PAW-PBE with dispersion correction](#)

*The Journal of Chemical Physics* **146**, 054702 (2017); 10.1063/1.4974921

---



# Unfolding DNA condensates produced by DNA-like charged depletants: A force spectroscopy study

C. H. M. Lima, M. S. Rocha, and E. B. Ramos<sup>a)</sup>

*Laboratório de Física Biológica, Departamento de Física, Universidade Federal de Viçosa, Ave. P. H. Rolfs s/n, CEP, 36570-900 Viçosa, Minas Gerais, Brazil*

(Received 10 October 2016; accepted 17 January 2017; published online 2 February 2017)

In this work, we have measured, by means of optical tweezers, forces acting on depletion-induced DNA condensates due to the presence of the DNA-like charged protein bovine serum albumin (BSA). The stretching and unfolding measurements performed on the semi-flexible DNA chain reveal (1) the softening of the uncondensed DNA contour length and (2) a mechanical behavior strikingly different from those previously observed: the force-extension curves of BSA-induced DNA condensates lack the “saw-tooth” pattern and applied external forces as high as  $\approx 80$  pN are unable to fully unfold the condensed DNA contour length. This last mechanical experimental finding is in agreement with force-induced “unpacking” detailed Langevin dynamics simulations recently performed by Cortini *et al.* on model rod-like shaped condensates. Furthermore, a simple thermodynamics analysis of the unfolding process has enabled us to estimate the free energy involved in the DNA condensation: the estimated depletion-induced interactions vary linearly with both the condensed DNA contour length and the BSA concentration, in agreement with the analytical and numerical analysis performed on model DNA condensates. We hope that future additional experiments can decide whether the rod-like morphology is the actual one we are dealing with (e.g. pulling experiments coupled with super-resolution fluorescence microscopy). *Published by AIP Publishing.* [<http://dx.doi.org/10.1063/1.4975103>]

## I. INTRODUCTION

DNA condensation or DNA compaction is a term usually used to describe a process in which disperse DNA molecules are compacted into tiny, nanometer-sized forms often presenting a globule, rod, or tours-like morphology.<sup>1</sup> In such a process, the micrometer-sized, worm-like DNA chain is folded in a highly dense and liquid-crystalline ordered structure, with a drastic reduction in its spanned volume.

*In vitro*, DNA condensation can be usually achieved by using cationic molecules with a charge equal or higher than +3 (cation-induced condensation)<sup>1,2</sup> or neutral polymers such as polyethylene-glycol (PEG) and monovalent salt ( $\psi$ -condensation).<sup>3</sup> In the former case, the positional correlation among the cationic ligands onto the DNA double-helix acts by promoting DNA segment-segment attraction resulting in the collapse of the DNA molecule,<sup>4</sup> whereas in the latter one, the condensing agent does not bind the double-helix and the compaction process is driven by the exclusion of the depletants surrounding the DNA segments, thus giving rise to attractive depletion-induced DNA segment-segment interactions.<sup>5</sup> Since the amounts of depletants usually needed to achieve DNA condensation are in the range of  $\sim 10\%$ – $30\%$  ( $w/w\%$ ), the solution conditions are termed “crowded.”<sup>6</sup>

An inverse scenario is presented, e.g., by the ejection of phage genomic DNAs from within its capsid into bacteria. The highly confined DNA chain is released into the cytosol and the bending and electrostatic energies which are

needed to confine the viral DNA inside its capsid are responsible for the ejection. It has also been shown that crowding can suppress partially or totally the DNA ejection from T4 phages into a neutral polymer (PEG) solution.<sup>7</sup> The ejection of phage DNA into bacteria is an example of a biological process which is, to some extent, related to pulling experiments performed with single DNA chains in PEG solutions where fractions of the condensed DNA contour length are pushed into a crowded environment:<sup>8</sup> here crowding plays both roles of keeping the condensate structure (keeping the chain confined within the condensate volume) and opposing the swell or release of the semi-flexible chain into the crowded solution, in such a way that, an external force is needed to unfold the condensate.

On the one hand, there is an abundant literature on force spectroscopy of cation-induced DNA condensates under several solution conditions showing, e.g., the well known stick-release pattern in the force-extension curves (a signature of this sort of condensate), the unfolding of its loops, and changes in the free energies involved.<sup>9–12</sup> On the other hand, very few experimental works have focused on the mechanics of depletion-induced DNA condensation in a crowded environment,<sup>13,14</sup> despite the known relative importance of crowding in the nuclear architecture and functioning in eukaryotic cells<sup>15</sup> (and references therein). More recently,<sup>16</sup> Langevin dynamics simulations were used to study the details involved in the folding/unfolding of torus and rod-like DNA condensates. Rod and torus-like condensates seem to have a different “finger-print” during the stretching, i.e., the force-extension curve is markedly different for these two morphologies.

<sup>a)</sup>Electronic mail: esio@ufv.br

To fill in this gap on the experimental side, we have measured the force-extension curve of DNA condensates induced by the BSA protein (bovine serum albumin), a DNA-like (negatively) charged protein, at a single molecule level, using optical tweezers to perform force spectroscopy. DNA-like charged protein-induced DNA condensation was initially proposed on theoretical grounds by de Vries<sup>17</sup> based on analytical and numerical calculations which took into account detailed protein-DNA interactions and later, observed experimentally by means of fluorescence microscopy by Yoshikawa *et al.*<sup>18</sup> From the measurements presented in this work, we have been able to find the experimental case where the stick-release behavior is not present during the condensate unfolding, as predicted for rod-like condensates under tension,<sup>16</sup> as well as to estimate the DNA segment-segment induced attractive interactions as a function of the BSA concentration.

The experimental setup and the procedure used to perform the measurements were described in detail previously.<sup>8,19,20</sup> In brief, our optical tweezers consist of a 1064 nm ytterbium-doped fiber laser (IPG Photonics) operating in the TEM<sub>00</sub> mode, mounted on a Nikon Ti-S inverted microscope with a 100× NA 1.4 objective. The tweezers are previously calibrated by using the Stokes force calibration procedure before the experiments. Once calibrated, the apparatus is used to trap the polystyrene bead attached to a DNA molecule. By moving the microscope stage using a piezoelectric actuator, we stretch the DNA while monitoring the changes of the bead position in the tweezers' potential well, using video-microscopy. In all experiments, we used  $\lambda$ -DNA ( $\sim 48\,500$  base-pairs,  $\sim 16.5\ \mu\text{m}$  contour length) in a Phosphate Buffered Saline (PBS) solution with  $[\text{NaCl}] = 125\ \text{mM}$  and  $\text{pH} = 7.4$ . Such an ionic strength was chosen based on the detailed phase diagram of BSA-DNA mixtures mapped as a function of both BSA concentration and solution ionic strength.<sup>18</sup> The BSA concentration ranged from 0% to 30% (w/w%) or equivalently, the solution osmotic pressure ranged within  $\approx 0 - 2\ \text{atm}$ <sup>21</sup> and the force needed to stretch the chain as a function of the DNA extension was measured. Unlike the osmotic stress experiments<sup>22</sup> in which a certain osmotic pressure is applied and the DNA-DNA inter-axial distances are measured, we here measure the force needed to pull the ends of a single DNA molecule apart to a certain distance against an applied osmotic pressure.

## II. RESULTS

We have performed stretching experiments on BSA-induced DNA condensates in both the low-force entropic regime and in the high-force enthalpic regime, thus probing the mechanics of initial/intermediate states as well as the mechanics of fully condensed DNA. In Fig. 1 we show the force-extension curves of BSA-induced DNA condensates obtained in the low-force entropic regime. Further analysis can be performed by fitting the force-extension curves to the Marko-Siggia Worm-Like Chain (WLC) model,<sup>23</sup> which is valid for  $F < 5\ \text{pN}$  (dashed lines in Fig. 1). From these fittings, one can extract the values of two basic mechanical properties of the semi-flexible DNA chain under crowding conditions in the entropic regime: the contour and persistence lengths.

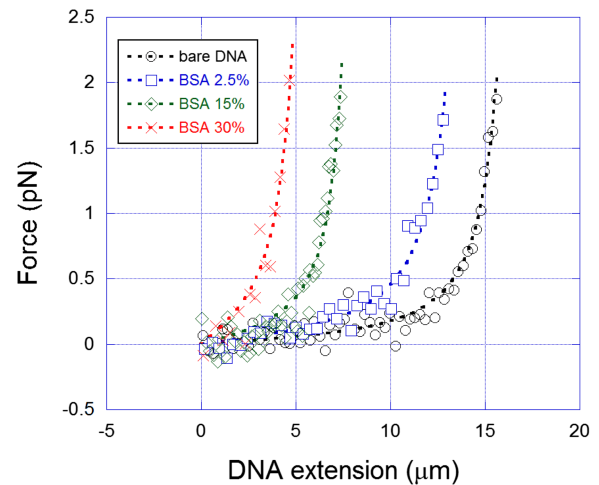


FIG. 1. Force-extension curves obtained in the low-force entropic regime for  $\lambda$ -DNA in the PBS buffer with  $[\text{NaCl}] = 125\ \text{mM}$  and various BSA concentrations ( $w/w\%$ ). Black  $\circ$ : bare DNA ( $C_{\text{BSA}} = 0$ ); blue  $\square$ :  $C_{\text{BSA}} = 2.5\%$ ; green  $\diamond$ :  $C_{\text{BSA}} = 15\%$ ; red  $\times$ :  $C_{\text{BSA}} = 30\%$ . Dashed lines: fittings to the WLC model, from where the apparent contour and persistence lengths can be determined.

Observe that the protein solution promotes an apparent (or effective) shortening and softening of the DNA molecule: due to the depletion-induced interactions, an effective attraction among the DNA segments sets in even at very low BSA concentrations  $\approx 2.5\% (w/w\%)$  reducing the orientational correlation among the DNA segments and therefore its persistence length. These forces measured at low BSA concentrations must be the pulling forces acting on intermediate, partially folded DNA condensates as seen under fluorescence microscopy by Yoshikawa *et al.*<sup>18</sup>

In Figs. 2 and 3 we synthesize, respectively, the behaviors of the apparent contour length  $L$  and the apparent persistence length  $A$  as a function of the BSA concentration in the solution, obtained from the WLC fittings. The behavior of these mechanical parameters is quite similar: they initially decrease from the bare DNA values, reaching minimum values at  $C_{\text{BSA}}$  between 20% and 30% ( $w/w\%$ ).

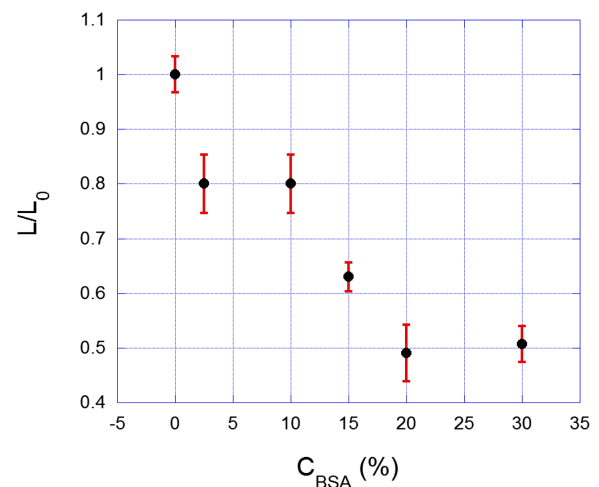


FIG. 2. Apparent contour length  $L$  (normalized by the full DNA contour length  $L_0$ ) of the DNA molecule as a function of the BSA concentration ( $w/w\%$ ) in the buffer (PBS with  $[\text{NaCl}] = 125\ \text{mM}$ ). Observe that  $L$  initially decreases from the bare DNA value, reaching a minimum at  $C_{\text{BSA}}$  between 20% and 30%.

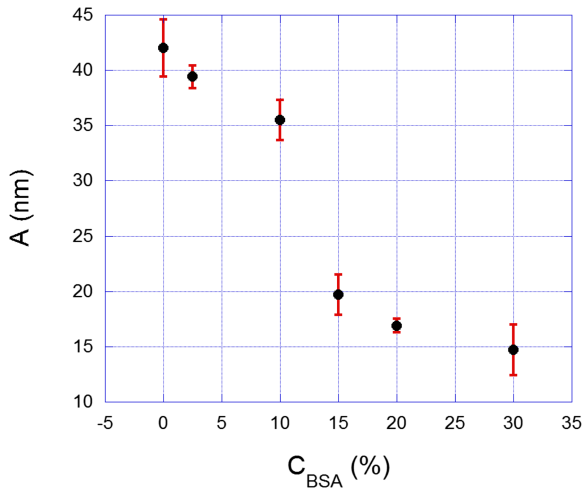


FIG. 3. Apparent persistence length  $A$  of the DNA molecule as a function of the BSA concentration ( $w/w\%$ ) in the buffer (PBS with  $[\text{NaCl}] = 125$  mM). Observe that  $A$  initially decreases from the bare DNA value, reaching a minimum at  $C_{BSA}$  between 20% and 30%.

In Fig. 4 we show typical force-extension curves obtained in the high-force enthalpic regime for four BSA concentrations. Observe that the curve corresponding to the bare  $\lambda$ -DNA ( $C_{BSA} = 0$ ) exhibits the well-characterized denaturation plateau which is related to the force-induced melting transition induced by stretching forces around  $\approx 65$  pN. The onset of such a plateau is shifted towards lower and lower extension as the BSA concentration is increased and is totally suppressed by 20% ( $w/w\%$ ) of BSA. This shift is in agreement with the fact that, as the bulk BSA concentration increases, larger is the DNA condensed contour fraction (in the sense that will be discussed below) and, moreover, only the uncondensed contour fraction is subject to the force-induced melting transition. Finally, as a last remark, no significant hysteresis has been found in the stretching-relaxation curve sets for any BSA concentration used in this work, which indicates that our stretching experiments were all performed under equilibrium conditions.

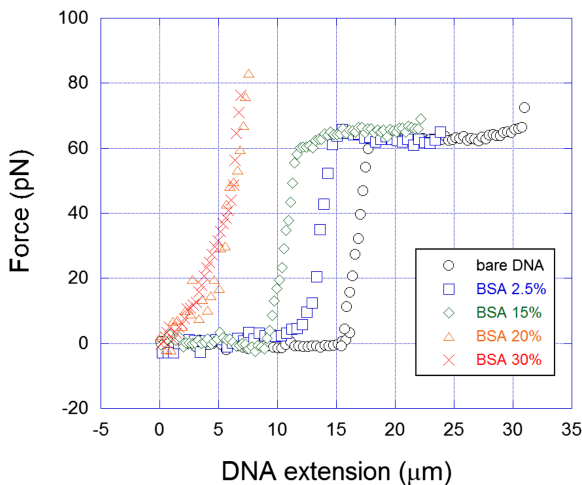


FIG. 4. Typical force-extension curves obtained in the high-force enthalpic regime for  $\lambda$ -DNA in the PBS buffer with  $[\text{NaCl}] = 125$  mM and various BSA concentrations ( $w/w\%$ ). Black  $\circ$ : bare DNA ( $C_{BSA} = 0$ ); blue  $\square$ :  $C_{BSA} = 2.5\%$  w/w; green  $\diamond$ :  $C_{BSA} = 15\%$ ; orange  $\triangle$ :  $C_{BSA} = 20\%$ ; red  $\times$ :  $C_{BSA} = 30\%$ .

### III. DISCUSSION

During the stretching and unfolding process, the pulling force exerted by the optical tweezers performs work ( $W_T$ ) which, to a first approximation, may be estimated as

$$W_T = W_{str} + \Pi_{osm} V_o, \quad (1)$$

$W_{str}$  being the work performed to stretch the chain, hindering undulations and aligning the unitary tangent vector along the tweezers' force direction.<sup>23</sup> The second term at the rhs of Eq. (1) is the osmotic work performed by the applied external force,  $\Pi_{osm}$  being the solution osmotic pressure and  $V_o$  the overlap volume. Therefore, the external work both reduces the chain condensed contour and stretches its uncondensed contour fraction. This is significant in the context of BSA-induced DNA condensates, since fluorescence images clearly show condensed and uncondensed fractions of the DNA contour coexisting within the same molecule, especially for BSA concentrations lower than 15%.<sup>18</sup> Again, to a first approximation, the force associated with the solution osmotic pressure (or work per unit length  $F_{osm}$ ) can be estimated as

$$F_{osm} \approx \Pi_{osm} \left( \frac{d_p + d_d}{2} \right)^2 - \left( \frac{d_d}{2} \right)^2, \quad (2)$$

$d_p$  and  $d_d$  being the protein and the DNA diameters respectively, whose values are  $\approx 7.0$  nm and  $\approx 2.4$  nm (within a more realistic approximation, the charge of both species would effectively increase these values<sup>17</sup>). To measure the osmotic work, we restrict ourselves to the analysis of the unfolding process which happens within the enthalpic regime, i.e., for forces higher than  $\approx 5 - 10$  pN. The idea behind this reasoning is the following: within the enthalpic regime, the bare DNA measured extension is nearly equal to the bare DNA contour length, since the thermal undulations along the chain are suppressed. Therefore, any change in the extension of the condensed DNA molecule relative to the extension of the bare DNA, within the high-force enthalpic regime, must be solely ascribed to the osmotic work. Note that such an approximation leaves not much room even for work contributions related to DNA secondary structural distortions, once the difference in relative extensions is measured for the same applied force.

The force  $F_{osm}$  associated with the osmotic pressure, according to Eq. (2), is expected to be constant, therefore, a constant, opposite, and equally intense applied external force  $F$  is needed to unpack the DNA condensed contour length, i.e., to bring condensed DNA segments into the crowded colloidal suspension. At this point, we need to introduce the concept of the condensed contour length. We are led to define and measure it as follows: for the same applied force  $F$ , we directly measure the bare DNA extension  $L_o$  and the condensed DNA extension  $L_{pro}$ . Assuming that the condensate's linear dimensions are much smaller than the bare DNA full contour length,<sup>18,24</sup> the condensed contour  $L_c$  is estimated as  $L_c = L_o - L_{pro}$ . Therefore, the DNA condensed contour fraction is given by  $L_o - L_{pro}/L_o$  and the DNA uncondensed contour fraction is given by  $L_{pro}/L_o$ .

In Fig. 5, we present the DNA condensed contour length fraction as a function of the applied force  $F$ : as we could expect,  $L_c$  decreases (although just slightly) with the increasing (not constant) external applied force at low BSA concentrations; at high protein amounts, changes in  $L_c$  are close to 20%. Thus,

forces as high as  $\approx 60$  pN applied on the DNA chain are unable to fully unpack the condensed segments, just as predicted by Cortini *et al.* for rod-like DNA condensates.

The change in the chain's free energy (from the condensed to the uncondensed state) may be estimated from the Gibbs-Duhem equation once the change in the condensed contour  $\Delta L_c(F)$  as a function of the applied external force  $F$  is known (at constant temperature),

$$\Delta\mu = - \int_{L_i}^{L_f} \Delta L_c(F) dF. \quad (3)$$

The resulting changes in the Gibbs free energy per unit length (measured in  $K_B T/\text{nm}$ ) are shown in Figure 6 along with the BSA concentration under which the unpacking process happens: the depletion-induced interactions vary linearly with the changes in the condensed contour length and with the BSA concentration as predicted, although the values found here are somewhat higher than those obtained numerically by de Vries.<sup>17</sup> Differences in protein charges and sizes, as well as in the ionic strength could explain part of this disagreement.

Recently, Langevin dynamics simulations have shown that the force-extension measurements of condensed semi-flexible chains may depend on the morphology of the condensate and can influence the dynamics of the unpacking process.<sup>16</sup> Particularly, the authors discuss the differences in stretching a torus and a rod-like DNA condensate, morphologies usually adopted by DNA condensates.<sup>24</sup> For the torus-like configuration, the authors found a stick-release pattern, already observed in pulling experiments of condensed DNA by multivalent cations such as spermine or spermidine.

On the other hand, for the rod-like configurations, the force-extension measurement is strikingly different. First, there is no stick-release pattern and more interestingly, the tensions used in their simulations are unable to unfold the condensate, i.e., to stretch the full contour of the DNA chain.

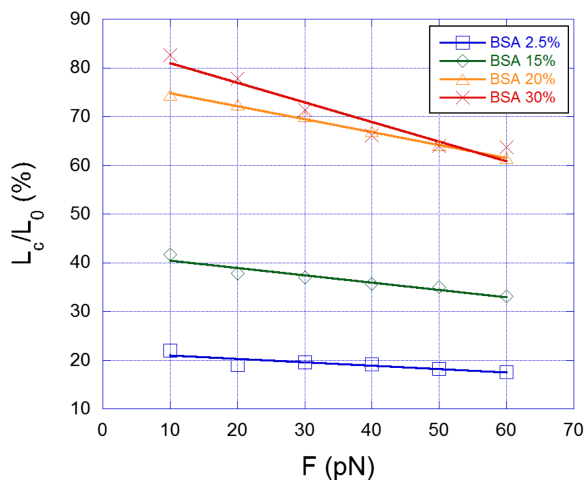


FIG. 5. Condensed contour  $L_c$  per unit length as a function of the applied force for  $F$  (pN) during the stretching of  $\lambda$ -DNA in the PBS buffer with  $[\text{NaCl}] = 125$  mM and different BSA concentrations ( $w/w\%$ ). Blue  $\square$ :  $C_{BSA} = 2.5\%$ ; green  $\diamond$ :  $C_{BSA} = 15\%$ ; orange  $\triangle$ :  $C_{BSA} = 20\%$ ; red  $\times$ :  $C_{BSA} = 30\%$ . The straight lines are linear fits whose values are used to estimate numerically the strength of the depletion-induced interactions. See the discussion below.

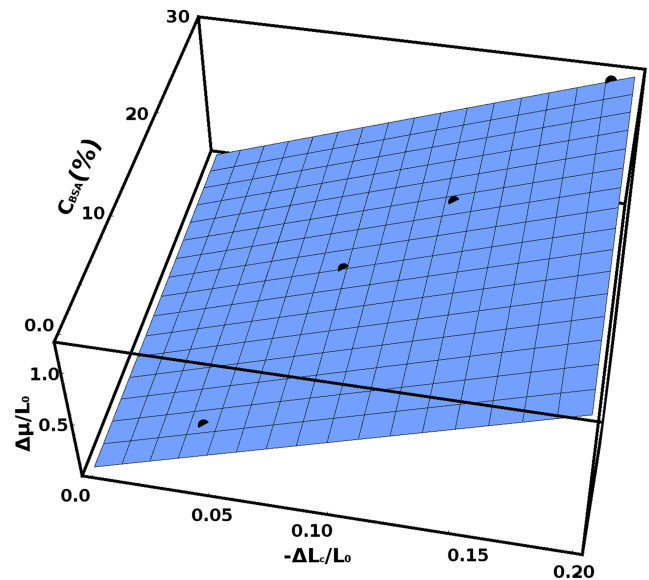


FIG. 6. Change in the chemical potential per unit length  $\Delta\mu/L_0$  (measured in  $K_B T/\text{nm}$ ) as a function of the changes in the DNA condensed contour fraction  $\Delta L_c/L_0$  and of BSA concentration ( $w/w\%$ ).

According to the authors, the rod-like structure is parallelly aligned to the applied tension at the beginning, which makes DNA segments slide on each other. At a certain point, once a given fraction of the DNA's contour is unpacked, the rod-like condensate tends to be oriented perpendicularly to the pulling force. In this case, the result is not the relative sliding of the DNA segments, in which one or a few chain segments are removed from the condensate each time, but to pull apart many DNA segments at once against the osmotic pressure.

This latter scenario seems to be the case found in our experiments, where a chain tethered at both ends is induced to collapse by the addition of BSA. Surprisingly, model-independent thermodynamics arguments provide us with quantitative insights into the force-induced unfolding process of a negatively charged semi-flexible chain in a crowded DNA-like charged environment which are in reasonable agreement with detailed numerical calculation, although for restricted changes in  $L_c$  and without the explicit presence of the depletant.<sup>16</sup>

A question which is raised is why, in our experiments, the chain would collapse preferentially forming rod-like DNA condensates. Analytical calculations have shown that, depending on the persistence length, a certain morphology is favored,<sup>25</sup> i.e., the semi-flexible chain may collapse into a globule, a rod, or a torus-like conformation. For increasingly more flexible chains, the rod and the globule-like morphologies are the stable states, whereas for chains with a higher persistence length, the toroidal conformation prevails.

The addition of BSA makes the chain effectively more flexible (see Figs. 1 and 4) which favors the rod-like structure instead of the torus-like conformation. Therefore, the initial effect of crowding would be the generic effect of worsening the solvent quality by whatever physical-chemical means, from a good solvent to a  $\theta$  solvent: reduced excluded-volume interactions and correlations among chain segments.<sup>26</sup> The reduced persistence length could be the cause of the preferential rod-like collapsed DNA state, since condensation would

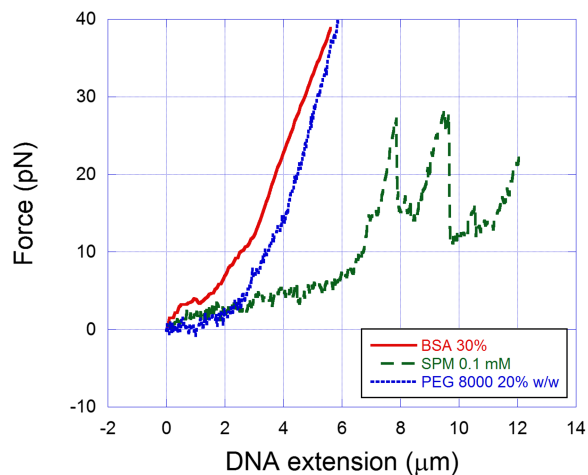


FIG. 7. Force-extension curves obtained for three different types of DNA condensates: BSA-induced condensates discussed here are obtained with  $C_{BSA} = 30\%$  (red solid line), cation-induced DNA condensates promoted by the tetravalent amine spermine (SPM) at 0.1 mM (green dashed line), and  $\psi$  DNA condensates promoted by the neutral polymer polyethylene-glycol (PEG) 8000 at 20% (blue dashed line).

involve less free energy in producing kinks along the chain contour. A scaling and numerical analysis of semi-flexible chains' persistence length in a crowded environment points at the same direction.<sup>27</sup> Of course, only additional numerical calculations just as those performed in Ref. 16 or additional stretching experiments coupled with super-resolution fluorescence microscopy or FRET on condensed DNA could settle the question. We hope to perform such experiments in the near future.

Finally, in order to compare the force-extension curves of DNA condensates obtained from a different solution condition, in Fig. 7 we show a comparison between the force-extension curves obtained for three different conditions: the BSA-induced condensates discussed here are obtained with  $C_{BSA} = 30\%$  (red solid line), cation-induced DNA condensates promoted by the tetravalent amine spermine (SPM) at 0.1 mM (green dashed line), and DNA  $\psi$ -condensates promoted by the neutral polymer polyethylene-glycol (PEG) 8000 at 20% (blue dashed line). The results for SPM- and PEG-induced condensates were previously obtained in Ref. 8.

These few experimental results, so far obtained for stretching curves of depletion-induced and cation-induced condensed DNA, seem to indicate a correlation between the interactions leading to condensation and the force-extension curves' profile. Clearly, more work is needed to prove/disprove this hypothesis.

## ACKNOWLEDGMENTS

This work was supported by the Brazilian Funding Agencies: Fundação de Amparo à Pesquisa do Estado de Minas Gerais (FAPEMIG), Conselho Nacional de Desenvolvimento Científico e Tecnológico (CNPq), and Coordenação de Aperfeiçoamento de Pessoal de Nível Superior (CAPES).

<sup>1</sup>V. A. Bloomfield, "DNA condensation by multivalent cations," *Biopolymers* **44**, 269–282 (1997).

<sup>2</sup>L. C. Gosule and J. A. Schellman, "Compact form of DNA induced by spermidine," *Nature* **259**, 333–335 (1976).

<sup>3</sup>L. S. Lerman, "A transition to a compact form of DNA in polymer solutions," *Proc. Natl. Acad. Sci. U. S. A.* **68**, 1886–1890 (1971).

<sup>4</sup>N. G. Jensen, R. J. Mashl, R. F. Bruinsma, and W. M. Gelbart, "Counterion-induced attraction between rigid polyelectrolytes," *Phys. Rev. Lett.* **78**, 2477–2480 (1997).

<sup>5</sup>S. Asakura and F. Oosawa, "On the interaction between two bodies immersed in a solution of macromolecules," *J. Chem. Phys.* **22**, 1255–1256 (1954).

<sup>6</sup>R. de Vries, "DNA compaction by nonbinding macromolecules," *Polym. Sci., Ser. C* **54**, 30–35 (2012).

<sup>7</sup>A. Evilevitch, L. Lavelle, C. M. Knobler, E. Raspaud, and W. M. Gelbart, "Osmotic pressure inhibition of DNA ejection from phage," *Proc. Natl. Acad. Sci. U. S. A.* **100**, 9292–9295 (2003).

<sup>8</sup>M. S. Rocha, A. G. Cavalcante, R. Silva, and E. B. Ramos, "On the effects of intercalators in DNA condensation: A force spectroscopy and gel electrophoresis study," *J. Phys. Chem. B* **118**, 4832–4839 (2014).

<sup>9</sup>C. G. Baumann, V. A. Bloomfield, S. B. Smith, C. Bustamante, M. D. Wang, and S. M. Block, "Stretching of single collapsed DNA molecules," *Biophys. J.* **78**, 1965–1978 (2000).

<sup>10</sup>Y. Murayama, H. Wada, and N. Sano, "Dynamic force spectroscopy of a single condensed DNA," *Europhys. Lett.* **79**, 1902–1910 (2007).

<sup>11</sup>A. Shirahata, T. J. Thomas, B. A. Todd, V. A. Parsegian, and D. C. Rau, "Attractive forces between cation condensed DNA double helices," *Bio-phys. J.* **94**, 4775–4782 (2008).

<sup>12</sup>B. van Den Broek, M. C. Noom, J. van Mameren, C. Battle, F. C. MacKintosh, and G. J. L. Wuite, "Visualizing the formation and collapse of DNA toroids," *Biophys. J.* **98**, 1902–1910 (2010).

<sup>13</sup>H. Ojala, G. Ziedaite, A. E. Wallin, Dennis, D. H. Bamford, and E. Haegstrom, "Optical tweezers reveal force plateau and internal friction in peg-induced DNA condensation," *Eur. Biophys. J.* **43**, 71–79 (2014).

<sup>14</sup>W. Xu and S. J. Muller, "Polymer-monovalent salt-induced DNA compaction studied via single-molecule microfluidic trapping," *Lab Chip* **12**, 647–651 (2012).

<sup>15</sup>S. Huet, C. Lavelle, H. Ranchon, P. Carrivain, J.-M. Victor, and A. Bancaud, "Relevance and limitations of crowding, fractal, and polymer models to describe nuclear architecture," *Int. Rev. Cell Mol. Biol.* **307**, 443–479 (2014).

<sup>16</sup>R. Cortini, B. R. Caré, J.-M. Victor, and M. Barbi, "Theory and simulations of toroidal and rod-like structures in single molecules DNA condensation," *J. Chem. Phys.* **142**, 1–9 (2015).

<sup>17</sup>R. de Vries, "Depletion-induced instability in protein-DNA mixtures: Influence of protein charge and size," *J. Chem. Phys.* **125**, 0149051 (2006).

<sup>18</sup>K. Yoshikawa, S. Hirota, N. Makita, and Y. Yoshikawa, "Compaction of DNA induced by like-charge protein: Opposite salt-effect against the polymer-salt-induced condensation with neutral polymer," *J. Phys. Chem. Lett.* **1**, 1763–1766 (2010).

<sup>19</sup>F. A. P. Crisafulli, E. C. Cesconetto, E. B. Ramos, and M. S. Rocha, "DNA-cisplatin interaction studied with single molecule stretching experiments," *Integr. Biol.* **4**, 568–574 (2012).

<sup>20</sup>E. C. Cesconetto, F. S. A. Junior, F. A. P. Crisafulli, O. N. Mesquita, E. B. Ramos, and M. S. Rocha, "DNA interaction with actinomycin d: Mechanical measurements reveal the details of the binding data," *Phys. Chem. Chem. Phys.* **15**, 11070–11077 (2013).

<sup>21</sup>K. A. S. Vincent, L. Vilker, and C. K. Colton, "The osmotic pressure of concentrated protein solutions: Effect of concentration and pH in saline solutions of bovine serum albumin," *J. Colloid Interface Sci.* **79**, 548–566 (1981).

<sup>22</sup>V. A. Parsegian, R. P. Rand, N. L. Fuller, and D. C. Rau, "Osmotic stress for the direct measurement of intermolecular forces," *Methods Enzymol.* **127**, 400–416 (1986).

<sup>23</sup>J. F. Marko and E. D. Siggia, "Stretching DNA," *Macromolecules* **28**, 8759–8770 (1995).

<sup>24</sup>U. K. Laemmli, "Characterization of DNA condensates induced by poly(ethylene oxide) and polylysine," *Proc. Natl. Acad. Sci. U. S. A.* **72**, 4288–4292 (1975).

<sup>25</sup>T. X. Hoang, A. Giacometti, R. Podgornik, N. T. T. Nguyen, J. R. Banavarand, and A. Maritan, "From toroidal to rod-like condensates of semiflexible polymers," *J. Chem. Phys.* **140**, 064902 (2014).

<sup>26</sup>P. G. de Gennes, *Scaling Concepts in Polymer Physics*, 1st ed. (Cornell University Press, Ithaca, 1979).

<sup>27</sup>S. Schobl, S. Sturm, W. Janke, and K. Kroy, "Persistence-length renormalization of polymers in a crowded environment of hard disks," *Phys. Rev. Lett.* **113**, 238302 (2014).